Automatic generation of biomechanical computational models of the complete thoracic and lumbar spine from magnetic resonance images

Joeri Kok[1], Yulia Shcherbakova[2], Tom Schlösser[2], Peter Seevinck[2,3], Tijl van der Velden[2,3], René Castelein[2], Keita Ito[1,2], Bert van Rietbergen[1]
[1]Eindhoven University of Technology, Eindhoven, Netherlands, [2]University Medical Center Utrecht, Utrecht, Netherlands, [3]MRIguidance BV, Utrecht, Netherlands
j.kok@tue.nl

Disclosures: J. Kok: None. **Y. Shcherbakova:** None. **T. Schlösser:** None. **P. Seevinck:** 3A; MRIguidance BV. **T. van der Velden:** 3A; MRIguidance BV. **R. Castelein:** None. **K. Ito:** 8; GlobalSpineJ. **B. Van Rietbergen:** None.

INTRODUCTION: Subject-specific morphometric and finite element modelling studies of the spine often rely on CT scans, but these do not provide much contrast for soft tissues. For full spine models, such images therefore are often complemented with MR images, but this requires making two scans and complex co-registration of the images. With emerging deep-learning (DL) methods it is now possible to derive synthetic CT (sCT) images from MR images to represent bone that can be combined with images representing soft tissues derived from the same MR images [1]. As such images are perfectly aligned and offer optimal contrast for bone and soft tissues, they also offer new opportunities for automated segmentation and meshing. In a recent study, we investigated a DL method for automatic segmentation of the IVD and vertebrae as well as a recently developed mesh morphing approach using a Bayesian coherent point drift (BCPD) affine registration method to generate FE meshes [2,3]. The aim of this study was to extend this approach to include facet joints and nuclei pulposi and to test the automated generation of subject-specific biomechanical models of the thoracic and lumbar spine.

METHODS: The study was approved by the local medical ethics committee (protocol ID 15-466). 3D sagittal T1-weighted in-phase, out-of-phase, fat, water, and T2-weighted MR scans were taken from 13 adult volunteers (Fig. 1; voxel size: 0.625×0.625×1 mm3; field of view: 420×420×100 mm3). For 4 volunteers additional T2-weighted scans were taken using compressed sensing, and a shortened sequence. sCT scans were generated from the T1-weighted images using a pre-trained DL algorithm (BoneMRI V1.6, MRIguidance BV). A DL network (nnU-Net [4]) was trained on the in-phase, out-of-phase, fat, and water scans of 6 subjects for automatic segmentation of the IVD and facet joints. nnU-Net was also trained on the standard 3D T2-weighted scans of 6 subjects for the segmentation of the NP. For segmentation of the vertebrae, a pre-trained DL network was selected [5,6]. Using the newly trained and pre-trained networks, a validation relative to manual segmentations was performed on 2 of the remaining subjects, one of which had a scoliotic deformity (Cobb angle ~30°). For the NP, validation was also performed on the additional compressed sensing and shortened sequences. A template mesh (GHBMC F05-P, Elemance, LLC) was morphed to fit the segmentations using a BCPD algorithm (Fig. 1). The template was aligned using rigid registration. The IVDs and vertebrae were morphed to their respective segmentations. For an accurate load transfer between vertebrae, the facet joints were separately included by registering disc-shaped meshes to the segmentations and connecting them to the morphed mesh.

RESULTS SECTION: Validating the networks resulted in Dice scores ranging from 0.81 (facet joints) to 0.96 (vertebrae) (Fig. 1). Individual vertebrae, IVDs, and facet joints were successfully registered and morphed to the segmentations for both subjects. 94% of the complete morphed healthy and scoliotic spine, were within 2 mm of the segmentations. Regions where this distance was larger than 3 mm occurred in the spinous and transverse processes. Mesh quality of the template and morphed mesh was similar with more than 96% of elements with a Jacobian larger than 0.5.

DISCUSSION: sCT imaging enables a unique segmentation of discs and vertebrae without the need for registering CT and MR images and avoiding radiation exposure. Training a DL network on high-resolution MR and sCT images resulted in good automatic segmentations of both bony and soft tissues, even in the case of scoliotic deformities. When trained on high-resolution scans, automatic NP segmentations work well even on accelerated sequences. The accuracy of the facet joint segmentation was slightly lower due to their small and thin nature. However, all facet joints were captured and their size and angle can be used to improve the finite element model accuracy. Morphing of the spine to the segmentations resulted in good quality meshes suitable for FE analysis. We conclude that the present workflow offers a unique possibility for fully automated accurate patient-specific mesh generation.

SIGNIFICANCE/CLINICAL RELEVANCE: By using synthetic CT, images with good contrast in bone and soft tissues can be derived from the same MR scan. Based on such images patient-specific models of the spine can be made fully automated, enabling the analysis of large cohorts.

REFERENCES: 1. Morbée et al., Eur J Radiol *2021;* 2. Kok et al. Frontiers Bioeng. (accepted); 3. Hirose, IEEE Trans. Pattern Anal. Mach. Intell. *2021;* 4. Isensee et al., Nat Methods *2021* 5. Payer et al., VISAPP conference *2020*; 6. Sekuboyina et al., Med. Image Anal. *2021*

ACKNOWLEDGEMENTS: This project is funded by the European Research Council (Grant no: 101020004).

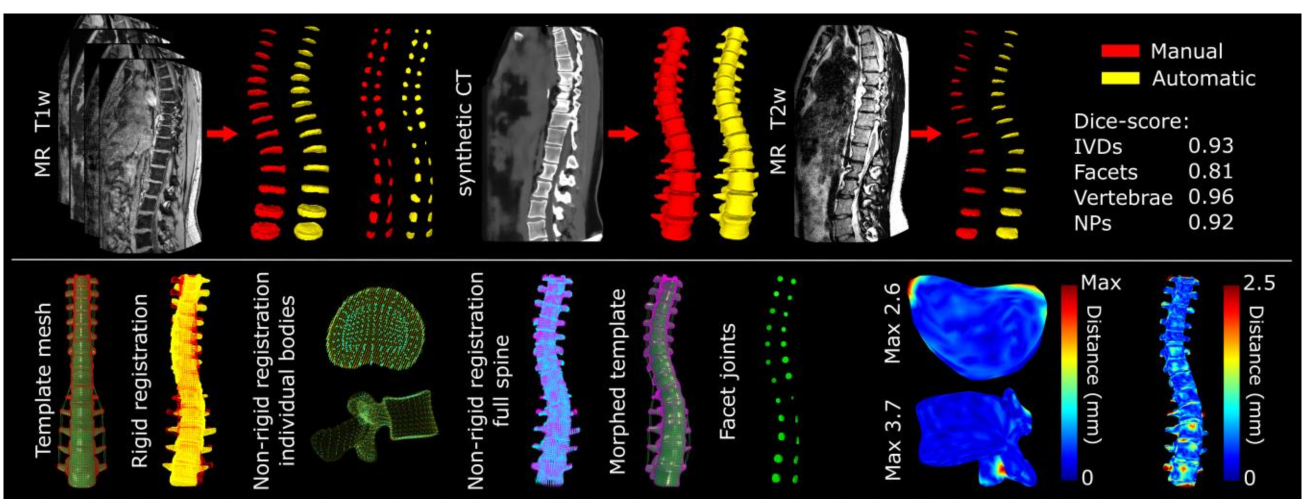

Figure 1. Workflow for the automatic generation of subject-specific finite element models for the evaluation of the biomechanical behavior of the spine. Top: Automatic segmentations of the IVDs and facet joints, vertebrae, and NPs are generated from the T1-weighted, sCT, and T2-weighted images, respectively. Dice-scores show similarity between manual and automatic segmentations. Bottom: Stepwise morphing for the generation of a subject-specific mesh. Distance measures from the surface of the resulting mesh to the surface of the segmentations are shown.